M HOAc and the solutions were diluted in 0.01 M phosphate buffered saline (pH 7.4) and used for bioassay. Local intraarterial infusion of the synthetic preparation of PHI induced a dose-dependent vasodilation as the natural PHI. The vasodilating potencies of both preparations were almost identical ($n = 4$) with respect to threshold doses (ca. 30–100 pmol min^{-1}) as well as maximal effects (ca. 10 nmol min^{-1}) (Figure 9).

Acknowledgment. The authors are grateful to Professor S. R. Bloom, Hammersmith Hospital, London, UK, for his generous gift of anti-natural PHI serum T33 and to Dr. K. Narita, Shizuoka College of Pharmacy, Shizuoka, Japan, for elemental analysis. This work was supported in part by Grants-in-Aid for Scientific Research No. 57370038 and No. 58580123 and for Cancer Research No. 57010034 from the Ministry of Education and Grant for Cancer Research No. 56-6 from the Ministry of Welfare, Japan.

Registry No. I, 92398-82-8; II, 91379-55-4; III, 92398-83-9; IV, 92398-84-0; V, 92398-85-1; VI, 92398-86-2; VII, 92398-87-3; VIII, 92398-88-4; IX, 92398-89-5; X·HCl, 92398-90-8; XI, 92398-91-9; XII, 92086-78-7; XIII, 92398-92-0; XIV, 92398-93-1; XV, 92420-10-5; XVI·HCl, 92398-94-2; XVII·HCl, 92420-22-9; Z-Ile-OSu, 3391-99-9; Z-Ile-NH_2, 86161-49-1; H-Ile-NH_2·HBr, 92398-95-3; Z-Leu-OSu, 3397-35-1; Z-Leu-Ile-NH_2, 82985-39-5; H-Leu-Ile-NH_2·HBr, 92398-96-4; Z-Ser-N_2H_3, 26582-86-5; Z-Ser-Leu-Ile-NH_2, 92398-97-5; H-Ser-Leu-Ile-NH_2·HOAc, 92398-98-6; Z-Glu(OBzl)-OH, 5680-86-4; Z-Glu(OBzl)-Ser-Leu-Ile-NH_2, 92398-99-7; H-Glu-Ser-Leu-Ile-NH_2·HOAc, 92399-01-4; H-Gln-OH, 56-85-9; Z-Leu-Gln-OH, 39802-26-1; H-Tyr-OMe·HCl, 3417-91-2; Boc-Lys(Z)-OH, 2389-45-9; Boc-Lys(Z)-Tyr-OMe, 92399-02-5; H-Lys(Z)-Tyr-OMe·TFA, 92399-03-6; Z-Lys(Z)-OH, 405-39-0; Z-Lys(Z)-Lys(Z)-Tyr-OMe, 92399-05-8; H-Leu-Glu-Ser-Leu-Ile-NH_2·HOAc, 92399-07-0; Z-Lys(Z)-Lys(Z)-Tyr-Leu-Glu-Ser-Leu-Ile-NH_2, 92399-08-1; H-Leu-Gln-Ser-Leu-Ile-NH_2·HOAc, 92399-10-5; Z-Lys(Z)-Lys(Z)-Tyr-Leu-Gln-Ser-Leu-Ile-NH_2, 92399-11-6; Z-Lys(Tos)-OH, 2362-45-0; Z-Lys(Tos)-Tyr-OMe, 92399-12-7; H-Lys(Tos)-Tyr-OMe·HCl, 92399-13-8; Z-Lys(Tos)-Lys(Tos)-Tyr-OMe, 92399-14-9; Z-Ser-Ala-OMe, 38428-20-5; Z-Leu-Ser-Ala-OMe, 92399-15-0; Z-Gln-N_2H_2-Boc, 2899-14-1; H-Gln-N_2H_2-Boc, 14485-97-3; Z-Leu-Gly-OH, 2706-38-9; Z-Leu-OH·dicyclohexylamine salt, 53363-87-4; H_2NNH-Boc, 870-46-2; Z-Leu-N_2H_2-Boc, 20898-09-3; H-Leu-N_2H_2-Boc, 2419-37-6; Z-Arg(NO_2)-OH, 2304-98-5; Z-Arg(NO_2)-Leu-N_2H_2-Boc, 92399-16-1; H-Arg-Leu-N_2H_2-Boc·2HOAc, 92399-18-3; Z-Phe-N_2H_2-Boc, 36374-63-7; H-Phe-N_2H_2-Boc, 36261-38-8; Z-Asp(OBzl)-OH, 3479-47-8; Z-Asp(OBzl)-Phe-N_2H_2-Boc, 68801-61-6; Z-Thr-Ser-OMe, 2488-24-6; Z-Thr-Ser-N_2H_3, 2488-25-7; H-Asp-Phe-N_2H_2-Boc, 68801-62-7; Z-Val-Phe-N_2H_2-Boc, 36254-67-8; H-Val-Phe-N_2H_2-Boc, 47555-32-8; Z-Gly-OH, 1138-80-3; Z-Gly-Val-Phe-N_2H_2-Boc, 92399-..-4; H-Gly-Val-Phe-N_2H_2-Boc, 92399-20-7; Z-Asp(OBzl)-Gly-Val-Phe-N_2H_2-Boc, 92399-21-8; Z-His-N_2H_3, 49706-31-2; H-Ala-OMe·HCl, 2491-20-5; Z-His-Ala-OMe, 28944-91-4; Z-His-Ala-N_2H_3, 61486-56-4; H-Asp-Gly-Val-Phe-N_2H_2-Boc, 92399-22-9; H-Lys(Tos)-Lys(Tos)-Tyr-Leu-Glu-Ser-Leu-Ile-NH_2·HOAc, 92399-24-1; H-Leu-Ser-Ala-Lys(Tos)-Lys(Tos)-Tyr-Leu-Glu-Ser-Leu-Ile-NH_2·HOAc, 92420-24-1; Z-Leu-Gly-Gln-N_2H_3·TFA, 92399-26-3; H-Leu-Gly-Gln-Leu-Ser-Ala-Lys(Tos)-Lys(Tos)-Tyr-Leu-Glu-Ser-Leu-Ile-NH_2·HOAc, 92399-28-5; H-Ser-Arg-Leu-Leu-Gly-Gln-Leu-Ser-Ala-Lys(Tos)-Lys(Tos)-Tyr-Leu-Glu-Ser-Leu-Ile-NH_2·HCl·HOAc, 92420-26-3; Z-Thr-Ser-Asp-Phe-N_2H_3·TFA, 92420-28-5; H-Thr-Ser-Asp-Phe-Ser-Arg-Leu-Leu-Gly-Gln-Leu-Ser-Ala-Lys(Tos)-Lys(Tos)-Tyr-Leu-Glu-Ser-Leu-Ile-NH_2·HCl·HOAc, 92399-30-9; Z-His-Ala-Asp-Gly-Val-Phe-N_2H_3·TFA, 92399-31-0; N^{α},N^{ϵ},N^{ϵ}-protected-PHI, 92399-32-1.

Supplementary Material Available: Listing of elemental analysis (4 pages). Ordering information is given on any current masthead page.

The Interconversion of the 5,6,7,8-Tetrahydro-, 7,8-Dihydro-, and Radical Forms of 6,6,7,7-Tetramethyldihydropterin. A Model for the Biopterin Center of Aromatic Amino Acid Mixed Function Oxidases

Gert Eberlein, Thomas C. Bruice,* R. A. Lazarus, Robert Henrie, and Stephen J. Benkovic*

Contribution from the Departments of Chemistry, University of California at Santa Barbara, Santa Barbara, California 93106, and The Pennsylvania State University, University Park, Pennsylvania 16802. *Received February 9, 1984*

Abstract: The 6,7-blocked pterins 6,6,7,7-tetramethyl-5,6,7,8-tetrahydropterin ($\mathbf{1}_{red}$), 6,6,7,7-tetramethyl-7,8-dihydropterin ($\mathbf{1}_{ox}$), and 5,6,6,7,7-pentamethyl-5,6,7,8-tetrahydropterin ($\mathbf{2}_{red}$) have been synthesized. $\mathbf{1}_{ox}$ represents the quinonoid product obtained upon $2e^-$ oxidation (electrochemical, Br_2) of $\mathbf{1}_{red}$. Two-electron oxidation of $\mathbf{2}_{red}$ yields $\mathbf{1}_{ox}$ rather than $\mathbf{2}_{ox}$ due to the rapid demethylation of the latter (the pseudo-first-order rate constant determined from elelectrochemical measurements at pH 5.9 is 1.4×10^{-2} s^{-1}). Solvolysis of $\mathbf{1}_{ox}$ yields the ring contracted imidazolone $\mathbf{3}_{ox}$ (Scheme III). The acid–base and spectral properties of $\mathbf{1}_{red}$ (Scheme I), $\mathbf{1}_{ox}$ (Scheme II), and $\mathbf{2}_{red}$ (Scheme IV) are described. The comproportionation equilibrium constant for the formation of the pterin radical $\mathbf{1}_{sem}$ has been determined by spectral and EPR measurements. The comproportionation constant for formation of $\mathbf{1}_{sem}$ from $\mathbf{1}_{red}$ and $\mathbf{1}_{ox}$ is much smaller ($\sim 10^7$-fold at pH 1.0 and $\sim 10^2$-fold at pH 7.0) than the like constants for flavin radical formation. The pH dependence of the redox potentials associated with $2e^-$ interconversion of $\mathbf{1}_{red}$ and $\mathbf{1}_{ox}$ has been determined and the like dependence of the $1e^-$ redox potentials for the interconversion of $\mathbf{1}_{red}$, $\mathbf{1}_{sem}$, and $\mathbf{1}_{ox}$ have been approximated. At scan speeds of 50 mV/s and at pH 5.9, the oxidation of $\mathbf{2}_{red}$ to $\mathbf{2}_{ox}$ can be shown to represent two $1e^-$ transfer steps in both anodic and cathodic sweeps. Nernst–Clark plots of potential vs. pH for **1** and **2** are provided (Figure 6). The mechanism of reaction of $\mathbf{1}_{red}$ and $\mathbf{2}_{red}$ with O_2 has been explored by comparing $\Delta G^{\ddagger}$ (from initial rates) to ΔG° values (electrochemical calculations) for $1e^-$ transfer from the tetrahydropterins to O_2. Since the difference $\Delta G^{\ddagger} - \Delta G^{\circ}$ is very small (13 kJ M^{-1}) and protons are not involved in the critical transition state, it is concluded that the transition state closely resembles the radical pairs $\{\mathbf{1}_{sem}O_2^{-}\cdot\}$ and $\{\mathbf{2}_{sem}O_2^{-}\cdot\}$ which must couple to provide 4a-hydroperoxypterins. The hydroperoxide moiety is consumed in the overall autocatalytic oxidation of $\mathbf{1}_{red}$ and $\mathbf{2}_{red}$.

The pterin-dependent aromatic hydroxylases phenylalanine hydroxylase, tyrosine hydroxylase, and tryptophane hydroxylase are involved in the synthesis of tyrosine and the neurotransmitters epinephrine and norepinephrine and the central nervous system transmitter serotonin. In the recycling of the cofactor (biopterin), the pterin ring structure is interconverted from its tetrahydro to a $2e^-$ oxidized quinonoid form shown as the para isomer in eq 1. It has been hypothesized that, in the cycle of eq 1, phenyl-

0002-7863/84/1506-7916$01.50/0

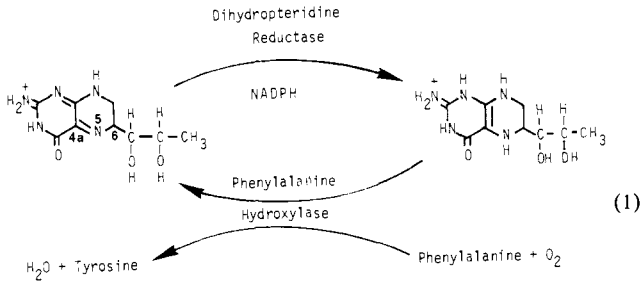

(1)

alanine hydroxylase bound tetrahydrobiopterin formed a hydroperoxide on reaction with O_2[1]in analogy to the 4a-hydroperoxyflavin species formed in model reactions[2a] and at the active site of flavoenzyme mixed function oxidases.[2b-h] Circumstantial evidence in support of this concept arose from the UV-vis spectral characteristics of a pterin product released from the apoprotein in the course of action of phenylalanine hydroxylase.[3] The structure of this product was tentatively assigned as a 4a,5-hydrate of quinonoid 7,8-dihydrobiopterin (analogous to the 4a,5-hydrate of flavin cofactors which arise via monooxygen transfer from the 4a-hydroperoxy flavin in flavin mixed function oxidase chemistry). This structure was confirmed by product studies with modified cofactors (5,6-diaminopyrimidines)[4] and by the results of both chemical model (5-deazapterin-4a-hydroxides and hydroperoxides) and enzyme studies.[5] Conclusive evidence for the proposed structure has come from enzymatic studies wherein the fate of a pterin cofactor enriched with ^{13}C at the C(4a) position was followed via ^{13}C NMR.[6a] The similarity in the structures of the biopterin and flavin 4a-hydroperoxides is obvious:

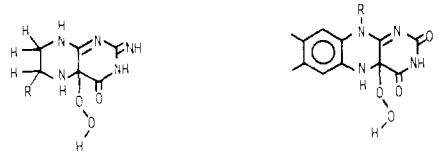

The mechanisms of the flavin hydroxylases and biopterin hydroxylases must differ in important aspects. Thus, the flavin hydroxylases are devoid of heavy metal requirements, but the biopterin enzymes are not. Studies of the tetrameric rat liver phenylalanine hydroxylase have confirmed that a tightly bound nonheme iron is necessary for the activity of the enzyme[7] and furthermore that the iron is in a 1:1 stoichiometry per subunit with the enzymic activity proportional to the iron content.[8] More recently it has been demonstrated that this iron is initially in a high-spin Fe^{3+} ($S = {}^5/_2$) state and that a reduction step involving the conversion of Fe^{3+} to Fe^{2+} is obligatory for activation of the enzyme.[9,10] This step can be carried out by various tetrahydropterins as well as dithionite with the latter stoichiometry being definitively established as 1 e^-/subunit suggesting that the pterin oxidation may proceed through discrete 1 e^- steps.[9]

Since the hydrogens located at the 6 and 7 positions of the pteridine ring are not involved in its activity as a cofactor[1,6b] and the presence of hydrogens at the 6-carbon results in unwanted isomerization (vide infra), we have synthesized and studied the 6,6,7,7-tetramethylpterins $\mathbf{1}_{red}$, $\mathbf{1}_{ox}$, and $\mathbf{2}_{red}$.[6c] In this paper we

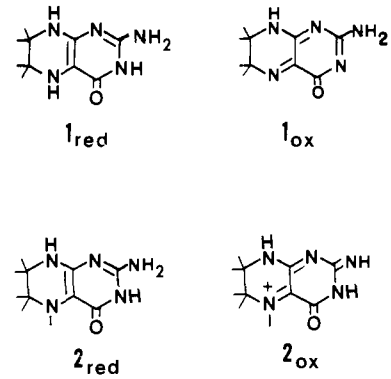

examine the acid-base chemistry and electrochemistry of these species, the stability of radical states, and the mechanism of the reaction of $\mathbf{1}_{red}$ and $\mathbf{2}_{red}$ with O_2. The radical $\mathbf{1}_{sem}$ is less stable than are flavin radical species. The radical $\mathbf{2}_{sem}$ is sufficiently stable to observe by conventional CV. As in the case of 1,5-dihydroflavin oxidation by O_2,[14a] the oxidation of $\mathbf{1}_{red}$ and $\mathbf{2}_{red}$ occurs by 1 e^- transfer to O_2 and coupling of the resultant $\mathbf{1}_{sem}O_2^{-}\cdot$ and $\mathbf{2}_{sem}O_2^{-}\cdot$ species to form unstable peroxides. The great instability of the pteridinium cation ($\mathbf{2}_{ox}$) has been established, and this instability has negated an obvious approach (eq 2) to the synthesis of the 4a-hydroperoxy adduct of $\mathbf{2}_{ox}$.

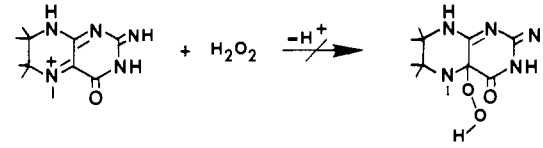

(2)

Experimental Section

5-Carbethoxy-2,2,3,3-tetramethyl-2,3-dihydropyrazin-6-one. A solution of 6.83 g (39.3 mmol) of diethyl ketomalonate and 4.60 g (39.7 mmol) of 2,3-dimethyl-2,3-diaminobutane[11] in 50 mL of absolute EtOH was stirred at room temperature for 45 h followed by refluxing for 7.5 h. The EtOH was evaporated to give a yellow oil, which was suspended in 50 mL of hexane and swirled vigorously to induce crystallization. The pale yellow solid was collected and dried overnight in vacuo at room temperature, affording 7.33 g (83%). Recrystallization from hexane gave colorless crystals, mp 118 °C. Anal. Calcd for $C_{11}H_{18}N_2O_3$ (M, 226.31): C, 58.58; H, 8.03; N, 12.38. Found: C, 58.18; H, 7.88; N, 12.31. IR (KBr) 3200, 3080 (lactam NH), 1740 (ester CO), 1690 (C=N), 1640 cm^{-1} (lactam CO). MS, m/e 226 (M^+) 1%, 169 [M - $NHC(CH_3)_2$] 6%, 153 [M - $CO_2C_2H_5$] 5%, 84 [$(CH_3)_2C{=}C(CH_3)_2$] 69%, 58 [NHC-

(1) Kaufman, S. *J. Biol. Chem.* **1959**, *234*, 2677-2682; **1964**, *239*, 332-338.

(2) (a) Bruice, T. C. *Acc. Chem. Res.* **1980**, *13*, 256-262. (b) Entsch, B.; Ballou, D. P.; Massey, V. *J. Biol. Chem.* **1976**, *251*, 2550. (c) Strickland, S.; Massey, V. *J. Biol. Chem.* **1973**, *248*, 2953. (d) Spector, T.; Massey, V. *J. Biol. Chem.* **1972**, *247*, 7123. (e) Hastings, J. W.; Balny, C.; LePeuch, C.; Dovzou, P. *Proc. Natl. Acad. Sci. U.S.A.* **1973**, *70*, 3468. (f) Hastings, J. W.; Balny, C. *J. Biol. Chem.* **1975**, *250*, 7288. (g) Massey, V.; Hemmerich, P. In "The Enzymes"; Boyer, P. D., Ed.; Academic Press: New York, 1976, Vol. XII, p 191. (h) Beaty, N. B.; Ballou, D. P. *J. Biol. Chem.* **1980**, *255*, 3817.

(3) Kaufman, S. In "Chemistry and Biology of Pteridines"; Pfleiderer, W., Ed.; de Gruyer: Berlin, 1975; p 291. Kaufman, S. "Iron and Copper Proteins"; Yasunobw, K. T., Mower, H. F., Hayaishi, O., Eds.; Plenum: New York, 1976; p 91.

(4) (a) Bailey. S. W.; Ayling, J. E. *Biochem. Biophys. Res. Commun.* **1978**, *85*, 1614-1621. (b) Bailey, S. W.; Ayling, J. E. In "Chemistry and Biology of Pteridines"; Kislink, R. L., Brown, G. M., Eds.; Elsevier: Amsterdam, 1979; pp 171-176. (c) Bailey, S. W.; Ayling, J. E. *J. Biol. Chem.* **1980**, *255*, 7774-7781. (d) Ayling, J. E.; Bailey, S. W. In "Oxygen and Oxy-Radicals in Chemistry and Biology"; Rodgers, M. A. J., Powers, E. L., Eds.; Academic Press: New York, 1981; pp 601-603. (e) Ayling, J. E.; Bailey, S. W. In "Flavins and Flavoproteins"; Massey, V., Williams, C. H., Eds.; Elsevier: Amsterdam, 1982; pp 294-297. (f) Bailey, S. W.; Weintraub, S. T.; Hamilton, S. M.; Ayling, J. E. *J. Biol. Chem.* **1979**, *254*, 5150-5154.

(5) (a) Moad, G.; Luthy, C. L.; Benkovic, S. J. *Tetrahedron Lett.* **1978**, 2271-2274. (b) Moad, G.; Luthy, C. L.; Benkovic, P. A.; Benkovic, S. J. *J. Am. Chem. Soc.* **1979**, *101*, 6068-6876. (c) Lazarus, R. A.; Dietrich, R. F.; Benkovic, S. J. *Biochemistry* **1981**, *20*, 6834-6891. (d) Lazurus, R. A.; Wallick, D. E.; Deitrich, R. F.; Gottschall, D. W.; Benkovic, S. J.; Gaffney, G. L.; Shiman, R. *Fed. Proc., Fed. Am. Soc. Exp.* **1982**, *41*, 2605.

(6) (a) Lazarus, R. A.; De Brosse, C. W.; Benkovic, S. J. *J. Am. Chem. Soc.* **1982**, *104*, 6869-6871. (b) Kwee, S.; Lund, H. *Biochim. Biophys. Acta* **1973**, *297*, 285-296. (c) Studies of 6,6-dimethylpterins have appeared: Bailey, S. W.; Ayling, J. E. *Biochemistry* **1983**, *22*, 1790-1798.

(7) Fisher, D. B.; Kirkwood, R.; Kaufman. S. *J. Biol. Chem.* **1972**, *247*, 5161-5167.

(8) Gottschall, D. W.; Dietrich, R. F.; Benkovic, S. J.; Shiman, R. *J. Biol. Chem.* **1982**, *257*, 845-849.

(9) Wallick, D. R.; Bloom, L. M.; Gaffney, B. J.; Benkovic, S. J. *Biochemistry* **1984**, *23*, 1295-1302.

(10) Marota, J.; Shiman, R. *Biochemistry*, in press.

(11) Sayre, R. *J. Am. Chem. Soc.* **1955**, *77*, 6689-6690.

(12) Schricks, B.; Bieri, J. H.; Viscontini, M. *Helv. Chim. Acta* **1978**, *61*, 2731-2738.

(13) Hubbard, A. T. *J. Electroanal. Chem.* **1969**, *22*, 165-174.

(14) (a) Eberlein, G. A.; Bruice, T. C. *J. Am. Chem. Soc.* **1983**, *105*, 6679-6684. (b) Paul, M. A.; Long, F. A. *Chem. Rev.* **1957**, *57*, 1-45.

$(CH_3)_2 + H^+]$ 100%. ^1H NMR ($CDCl_3$) δ 4.32 (q, 2, J = 7, CH_2CH_3), 1.35 (t, 3, J = 7, CH_2CH_3), 1.28 and 1.25 (s, 12, $C(CH_3)_2$).

5-Carbethoxy-2,2,3,3-tetramethyl-2,3,4,5-tetrahydropyrazin-6-one. A mixture of 7.33 g (32.4 mmol) of the dihydropyrazinone and 0.50 g of 10% Pd/C in 125 mL of absolute EtOH was hydrogenated at 40 psi (Parr shaker) for 3 h. After filtration through a Millipore filter, the solution was concentrated to dryness to yield 7.20 g (97%) of colorless crystalline product. Recrystallization from hexane gave the analytical sample, mp 118–122 °C. Anal. Calcd for $C_{11}H_{20}N_2O_3$ (M, 228.29): C, 57.87; H, 8.83; N, 12.27. Found: C, 57.91; H, 8.71; N, 12.36. IR (KBr) 1730 (ester CO), 1660 cm^{-1} (lactam CO). MS, m/e 228 (M^+) 7%, 226 (M – 2) 8%, 171 [M – $NHC(CH_3)_2$] 18%, 155 [M – $CO_2C_2H_5$] 13%, 84 [$(CH_3)C{=}C(CH_3)_2$] 26%, 58 [$NHC(CH_3)_2 + H^+$] 100%. Exact mass calcd for $C_{11}H_{20}N_2O_3$ 228.1474, found 228.1473.

5-Carbethoxy-6-ethoxy-2,2,3,3-tetramethyl-2,3,4,5-tetrahydropyrazine. A solution of 7.20 g (31.6 mmol) of the pyrazin-6-one and 50 mmol of triethyloxonium tetrafluoroborate in 110 mL of anhydrous CH_2Cl_2 was stirred under N_2 for 27 h at room temperature. The dark solution was treated with 40 mL of ice cold 25% aqueous K_2CO_3 for 15 min, filtered from precipitated KBF_4, and the layers separated. The CH_2Cl_2 layer was dried over anhydrous Na_2SO_4 and purified by filtration through 230–400 mesh silica gel 60 (E. Merck; 150 mL medium sintered glass funnel) eluting with 5% MeOH–CH_2Cl_2. The fractions which contained no starting material by TLC were pooled and evaporated to give a light yellow oil (7.35 g, 91%), which was used directly in the condensation with guanidine. MS, m/e 256 (M^+), 0.3%, 254 (M – H_2) 3.3%, 199 [M – $NHC(CH_3)_2$] 3.4%, 183 [M – $CO_2C_2H_5$] 4.4%, 171 [M – $MHC(CH_3)_2$ – C_2H_4] 14.3%, 84 [$(CH_3)_2C{=}C(CH_3)_2$] 32.7%, 58 [$NHC(CH_3)_2$ + H^+] 100%. Exact mass calcd for $C_{13}H_{24}N_2O_3$ 256.1786, found 256.1795.

6,6,7,7-Tetramethyl-5,6,7,8-tetrahydropterin (1_{red}). A mixture of 22.6 mmol of NaOEt (from 0.520 g Na), 2.17 g (22.7 mmol) of dry guanidine, HCl, and 4.73 g (18.5 mmol) of the 6-ethoxytetrahydropyrazine in 30 mL of dry DMF was heated to 130–140 °C (oil bath) under N_2 for 48 h. Concentrated HCl (20 mL) was added and the mixture evaporated to dryness. The dark residue was dissolved in 50 mL of 0.1 N HCl, loaded onto a 2.5 × 29 cm Dowex 50W-X4 (100–200 mesh) column, and eluted with 450 mL of 1 N HCl followed by 1575 mL of 2 N HCl (22-mL fractions). Fractions were assayed spectrophotometrically at 264 nm in 0.1 N HCl. Peak fractions were pooled and concentrated to give a yellow solution, which was decolorized by hydrogenation over 0.5 g of 10% Pd/C at 40 psi for several hours (impurity with λ at 295 nm (0.1 N HCl) removed). Filtration and evaporation to dryness gave a pale yellow solid, which was crystallized from a mixture of 0.6 mL of concentrated HCl, 10 mL of absolute EtOH, and 80 mL of absolute Et_2O,[12] yielding 1.24 g (19% based on M_r 355) of white solid after drying overnight at room temperature in vacuo. UV (0.1 N HCl) λ_{max} 264 (13 940 M^{-1} cm^{-1}). 360-MHz ^1H NMR (0.1 N DCl/D_2O, internal DSS) δ 1.45 (br s, 6, CH_3), 1.36 (s, 6, CH_3). Anal. Calcd for $C_{10}H_{17}N_5O{\cdot}2.3HCl{\cdot}0.1EtOH{\cdot}2.4H_2O$ (M_r 354.99): C, 34.51; H, 7.01; N, 19.73; Cl, 22.97. Found: C, 34.60; H, 6.34; N, 19.75; Cl, 22.56.

6,6,7,7-Tetramethyl-7,8-dihydropterin (1_{ox}). 6,6,7,7-Tetramethyltetrahydropterin dihydrochloride (194 mg; 0.66 mmol) was dissolved in 10 mL of 0.1 N HCl. A solution of 0.1 mL of Br_2 (1.95 mmol) in 10 mL of 0.1 N HCl was added. The oxidized pterin was formed immediately and purified in the following way: A column (1-cm diameter) containing 17 mL of Dowex 50W-X4 ion exchange was washed with 100 mL of 2 N HCl, 100 mL of 1 N HCl, and 100 mL of 0.1 N HCl. The reaction solution was added to the column followed by washing with 100 mL of 0.1 N HCl until the effluent was colorless. The product was then washed off the column with 50 mL of 1 N HCl. The yellow-green fraction contained 147 mg (89%) of pure monoprotonated product. The water was removed by rotary evaporation, and the moist crystals were dried over NaOH under vacuum. Brown-yellow crystals remained. UV (1 N $HClO_4$) λ_{max} [ϵ (M^{-1} cm^{-1})]: 341 (3600), 257 (7100), 210 (10500). MS (200 °C; chemical ionization; CH_4; 400 eV) 250 ($M^+ + 29$) 5%, 224 ($M^+ + 3$) 12%, 223 ($M^+ + 2$) 10%, 222 ($M^+ + 1$) 24%, 206 (M^+ – NH) 2%, 163 (M^+ – NHCONH) 9%. MS (200 °C; EI; 70 eV) 221 (M^+) 3%, 207 (M^+ – CH_2) 7%, 206 (M^+ – NH) 5%, 163 (M^+ – NHCONH) 100%.

5,6,6,7,7-Pentamethyl-5,6,7,8-tetrahydropterin (2_{red}). A suspension of 98 mg (0.29 mmol, M_r 341) of **1**, 120 mg of 10% Pd/C, 20 mL of 1.0 N HCl, and 4 mL of 37% formaldehyde was hydrogenated at 20 psi for 15 h at room temperature (Parr shaker). The catalyst was removed by filtration (Millipore) and washed with 5 mL of 6 N HCl. The filtrates were rotary evaporated to a white semisolid, which was triturated with a solution of 0.6 mL of concentrated HCl in 10 mL of absolute EtOH. A white solid (paraformaldehyde) was removed by filtration and 80 mL of anhydrous Et_2O added to the filtrate. The product separated as a colorless glass, which was dissolved in ca. 3 mL of 1 N HCl and passed over a 26-cm column of Dowex 50W-X4 (100–200 mesh, 26 mL volume), eluting with 1 N HCl (60 mL) followed by 2 N HCl (700 mL). Fractions (7 mL) were collected and assayed spectrophotometrically at 264 nm in 1 N HCl. The peak was pooled and evaporated to a white solid, which was dried overnight in vacuo. UV (0.1 N HCl) λ_{max} 264, 219; OD_{219}/OD_{264} = 1.24. 60-MHz ^1H NMR (0.1 N DCl/D_2O, DSS) δ 3.30 (s, 3, N – Me), 1.55 (s, 6, 6-Me), 1.48 (s, 7, 7-Me). Anal. Calcd for $C_{11}H_{19}N_5O{\cdot}2HCl{\cdot}H_2O$: C, 40.25; H, 7.06; N, 21.34; Cl, 21.60. Found: C, 40.20; H, 7.23; N, 21.15; Cl, 21.43.

Proton NOE measurements were obtained by difference of the free induction decays (FIDS) collected on and off resonance, employing a standard microcomputer sequence provided by Bruker Instruments. The NOE sample was prepared by dissolving 2_{red} in 0.1 N DCl and deoxygenated by several freeze–thaw cycles under vacuum before being sealed in an NMR tube. Proton enhancements of 6.0 and 8.0 were observed for the CH_3 groups at 1.48 and 1.55 ppm, respectively, upon irradiation of the CH_3–N at 3.30 ppm. No NOE was observed in the absence of irradiation at CH_3–N. Methylation thus is assigned to N-5 rather than N-2.

2-Amino-5,5,6,6-tetramethyl-5,6-dihydroimidazo[4,5-*b*]pyrazine (3_{ox}). To a solution of 112 mg (0.315 mmol) of 1_{red} in 60 mL of 0.1 M $K_2PO_4^-/KPO_4^{2-}$ buffer, pH 6.8, was added 15 μL (0.29 mmol) of Br_2 in 5 mL of EtOH. A bright yellow solution of the quinonoid form was immediately obtained, which was stirred for 4 days at room temperature open to air (final pH 6.55). Alternatively, the quinonoid form was generated by bubbling oxygen through the solution for 4 h. The water was evaporated and the residue stirred overnight with 60 mL of *t*-BuOH. After filtration from buffer salts, the *t*-BuOH was lyophilized and the residue triturated with ice cold CH_3CN, affording 28 mg (46%) of yellow imidazopyrazine. Recrystallization from CH_3CN gave the analytical sample as a dihydrate, mp 164–195 °C dec, with darkening from ca. 150 °C. Anal. Calcd for $C_9H_{15}N_5{\cdot}2H_2O$ (M_r 229.28): C, 47.14; H, 8.35; N, 30.55. Found: C, 47.32; H, 8.16; N, 30.80. 360-MHz ^1H NMR (D_2O, internal DSS) one sharp singlet, 1.26. MS, m/e 193 (M^+) 25.7%, 178 (M – CH_3) 8.2%, 163 (M – $2CH_3$) 2.1%, 136 [$C{\equiv}NC(CH_3)_2C(CH_3)_2N{\equiv}C$] 11.2%, 109 [$C{\equiv}NC(CH_3)_2C(CH_3){=}CH_2$] 9.9%, 84 [$(CH_3)_2C{=}C(CH_3)_2$] 6.0%, 68 [$C{\equiv}NC(CH_3)_2$] 17.9%, 58 [$NHC(CH_3)_2$ + H^+] 41.6%. UV (0.1 N HCl) λ_{max} 274 (23 240), 283 sh (21 660), 296 sh (10 900). UV (0.1 M KPO_4, pH 6.8) λ_{max} 270 (20 860), 282 sh (16 700), 297 sh (6880). Exact mass calcd for $C_9H_{15}N_5$ 193.1327, found 193.1327. ^{13}C NMR (D_2O, DSS internal) 182.1 (C2), 163.4 (C3a,7a), 61.6 (C5,6), 26.1 (5,5,6,6-Me).

Preparative Electrochemical Oxidation of 6,6,7,7-Tetramethyl-5,6,7,8-tetrahydropterin Dihydrochloride (1_{red}). 1_{red} (0.3 mg, 1.03 mmol) in 16 mL of 1 M $HClO_4$ was electrolyzed under stirring at 180 mV below the negative redox potential of the pterin with an initial current of 3.1 × 10^{-1} C s^{-1} with use of coiled Pt wire (0.5-mm diameter, 60-mm long) as working electrode. The auxiliary electrode (Pt wire, coiled, 0.5-mm diameter, 100-mm long, 1 M NaCl as electrolyte) was separated from the reaction solution by a G4 glass frit (50-mm^2 surface). The silver reference electrode contained in 1 M NaCl, $Ag^+/AgCl$, was also separated from the reaction solution by a ground glass joint. The reaction was completed within 2 h with a remaining current of 1.6 × 10^{-7} C s^{-1}. The yield of 1_{ox} was quantitative. The solution of 1_{ox} so obtained was employed directly in the determination of spectra and pK_a values.

Analytical Electrochemistry. The reduction potentials for pterin (**1**) were determined from solutions containing 1 mL of 2 M $NaClO_4$, 1 mL of Me_2SO, 0.05 mL of 2 M acetate buffer (pH 5.8), 1 mL of 2 M $NaClO_4$, 1 mL of Me_2SO, 0.1 mL of 1 M $HClO_4$ (pH 1.90); 1 mL of 8 M $NaClO_4$, 0.9 mL of 8 M $HClO_4$, 0.1 mL of 8 M $HClO_4$ containing 1.29 × 10^{-2} M pterin (H_0 = –1.72); 0.5 mL of 8 M $NaClO_4$, 1.4 mL of 8 M $HClO_4$, 0.1 mL of 1 M $HClO_4$ containing 1.29 × 10^{-2} M pterin (H_0 = –4.33).

The reduction potentials for the pterin (**2**) reported herein were determined by use of thin-layer cyclic voltammetry techniques of Hubbard,[13b] and the number of electrons transferred was determined from both the peak height and the integrated surface under the peak as described previously.[14a] Scanning was from negative to positive potential employing a 0.75 V scan range at a sensitivity of 0.01 mA. The analytical electrochemistry was carried out in 2 mL of reaction solutions employing the following buffers (μ = 0.95–1.0): 1.4 mL of 1 M $HClO_4$, 0.1 mL of 1.24 × 10^{-2} M 2_{red} in Me_2SO (H_0 = –0.22); 1.7 mL of 1 M $NaClO_4$, 0.2 mL of 0.5 M sulfate buffer, 0.1 mL of 1.29 × 10^{-2} M 2_{red} in Me_2SO (pH 1.22); 1.85 mL of 1 M $NaClO_4$, 0.05 mL of 2 M acetate buffer, 0.1 mL of 1.29 × 10^{-2} M 2_{red} in Me_2SO (pH 4.01); 1.7 mL of 1 M $NaClO_4$, 0.2 mL of 0.5 M phosphate buffer, 0.1 mL of 1.29 × 10^{-2} M 2_{red} in Me_2SO (pH 5.9); 1.8 mL of 1 M $NaClO_4$, 0.1 mL of 2 M tris/$HClO_4$ buffer, 0.1 mL of 1.29 × 10^{-2} M 2_{red} in Me_2SO (pH 8.05). One-tenth of a milliliter of a pterin stock solution, 1.29 × 10^{-2} M in Me_2SO (stored in refrigerator at –22 °C), was added to obtain a final concentration in pterin of 6.45 × 10^{-4} M. The reference employed was

AgCl/1 M NaCl (reference potential 0.225 V vs. NHE at 25 °C). All potentials are given vs. NHE. The Pt electrode was I_2 coated prior to use by dipping the electrode in aqueous 1 M NaI solution and thoroughly rinsed with water. The scan speed employed for conventional cyclic voltammetry was 100 mV/s.

pK_a determinations with $\mathbf{1}_{ox}$ were carried out as follows: $\mathbf{1}_{red}$ was oxidized electrochemically in a titration cell equipped with stirrer in a Cary 15 UV-vis spectrophotometer at $H_0 = -0.22$. The path length of the cell was 3.335 cm. The starting concentration was approximately 3×10^{-5} M, and the volume of the solution was 16 mL. The pH was determined with a combined glass electrode after each addition of base. The UV-vis spectrum was scanned after each 0.3 to 0.5 pH unit increase. After reaching pH 13 the solution was titrated back to pH 1 with concentrated sulfuric acid and the starting spectrum and final spectrum were compared. Concentrated solutions of acid and base were employed for this titration to keep the increase in volume to a minimum.

For $\mathbf{1}_{ox}$ the change in absorbance with change in acidity was followed at 258 nm (pK_a = −3.68), 260 and 310 nm (pK_a = 5.23), and 310 nm (pK_a = 10.63). For the pK_a in the H_0 range concentrated sulfuric acid was added and the H_0 calculated after a table from Paul and Long.[14b] The UV-vis spectrum was scanned after each 0.3- to 0.5 H_0 unit change.

The pK_a of $\mathbf{1}_{red}$ was determined in a similar way as described for $\mathbf{1}_{ox}$; however, the titrations were carried out in a Cary 15 spectrophotometer with the sample compartment sealed in a glovebox under nitrogen. The oxygen concentration in the glovebox was $\sim 5 \times 10^{-8}$ M. The change in the UV-vis spectrum with change in acidity was followed at 297 nm (pK_a = 10.66), 297 and 265 nm (pK_a = 5.69), 265 nm (pK_a 1.27), and 280 nm (pK_a = −6.01). The pK_a of $\mathbf{2}_{red}$ was determined in a similar way as for the pK_a of $\mathbf{1}_{red}$. The change of absorbance was monitored at 264 nm (pK_a = 5.74) and at 310 nm (pK_a = 11.14).

Determination of the Equilibrium Constant for the Formation of $\mathbf{1}_{sem}$. A solution 1×10^{-3} M in $\mathbf{1}_{red}$ and a separate solution 1×10^{-3} M in $\mathbf{1}_{ox}$, both in 1 M HCl, were placed in separate compartments of two tandem cuvettes, path length 0.438/0.439; 0.438/0.437 cm. One cuvette was placed in the reference compartment and the other in the sample compartment of a Cary 118 spectrophotometer. The base line was set at zero from 800 to 300 nm at an absorbance scale of 0–0.1. The spectrum was run after mixing the contents of the sample cell. For the calculation of the concentration of $\mathbf{1}_{sem}$ (Results) the increase in A_{475} was determined.

Kinetics. In the reaction of $\mathbf{1}_{red}$ or $\mathbf{2}_{red}$ with oxygen, air-saturated buffer solutions, 2 M acetate (pH 4.6), 0.5 M sulfate (pH 1.85), and 0.5 M phosphate (pH 6.9) were placed in a cuvette and thermally equilibrated in the cell compartment of the spectrophotometer at 30 ± 0.2 °C. $\mathbf{1}_{red}$ (0.1 mL, 6.00×10^{-4} M in water) was added and the appearance of $\mathbf{1}_{ox}$ followed at 343 nm (acetate buffer), 217 nm (phosphate buffer), 260 nm (carbonate buffer, pH 9.9), 258 nm (tris, pH 7.80), or 343 nm (1 M $HClO_4$, H_0 −0.22).

In the reaction of $\mathbf{2}_{red}$ with oxygen in *tert*-butyl alcohol, 3 mL of water-free and anaerobic *tert*-butyl alcohol were mixed with 0.01 mL of 6.87×10^{-3} M $\mathbf{2}_{red}$ in water-free DMF. The initial spectrum was run and air was admitted to the contents of the cuvette. The change in spectrum at 250 nm was followed.

Hydrogen peroxide was determined by withdrawing 0.05 mL from a cuvette containing the reaction solution and placing it in a freshly mixed solution of 3 mL of 0.1 M NaI in 95% ethanol, 0.06 mL of a solution 0.1 M in acetic acid, and 1 M in sodium acetate (the assay solutions are stable when stored separately at 4 °C) and 1 mL of water. The pseudo-first-order rate constant for the oxidation of I^- by H_2O_2 was 7.01×10^{-4} s^{-1} (9.6×10^{-3} M^{-1} s^{-1}) in the assay solution employed. Appearance of I_3^- was followed at 358 nm (ϵ = 25 000). The reference cuvette contained an equivalent, H_2O_2-free mixture. Since the maximum absorbance disappears again with a first-order rate constant of $\sim 4.9 \times 10^{-6}$, the maximum I_3^- formation was extrapolated to time 0 (~3.2% additional absorbance).

The ESR spectrum of $\mathbf{1}_{rad}$ was recorded on a Bruker electron spin resonance spectrometer ER 200 D-SRC in connection with a Nicolet signal averager. The quantitative measurement of the spin number was taken relative to a ruby reference (Cr^{3+} in Al_2O_3). The g factor was determined relative to a DPPH standard. The sweep width was 150 G. The sweep time was 10 s. The sweep number was 47 at J_0 = 9.48 GHz, H_0 = 3315.0 G. The two samples examined were 7×10^{-3} M in both $\mathbf{1}_{ox}$ and $\mathbf{1}_{red}$ dissolved in a solvent 14.26 M in methanol and 7.42 M in acetic acid and 1.5×10^{-2} M in both $\mathbf{1}_{ox}$ and $\mathbf{1}_{red}$ dissolved in trifluoroacetic acid.

Results

Acid–Base Chemistry of $\mathbf{1}_{red}$ and $\mathbf{1}_{ox}$. The pK_a values associated with the acid–base chemistry of $\mathbf{1}_{red}$ and $\mathbf{1}_{ox}$ have been determined by spectral titration in aqueous solution (Experimental Section). The UV-vis spectra of $\mathbf{1}_{red}$, at various pH values, are given in

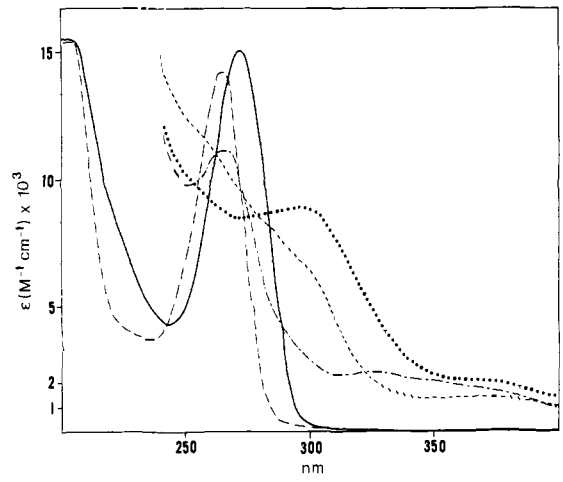

Figure 1. UV-vis spectra of the acid–base species of $\mathbf{1}_{red}$ in aqueous solution at various pH. [$\mathbf{1}_{red}$] ~ 1.5×10^{-5} M. (—) $\mathbf{1}_{red}H_3^{3+}$ (H_0 = −9); (--) $\mathbf{1}_{red}H_2^{2+}$ (H_0 = −3.8); (-·-) $\mathbf{1}_{red}H^+$ (pH 3.9); (···) $\mathbf{1}_{red}$ (pH 8.8); (---) $\mathbf{1}_{red}^-$ (pH 13.0).

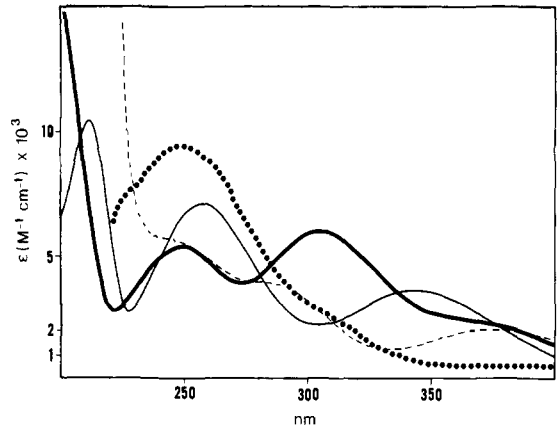

Figure 2. UV-vis spectra of the acid–base species of $\mathbf{1}_{ox}$ in aqueous solution at various pH. (···) $\mathbf{1}_{ox}H_2^{2+}$ (H_0 = −4.22, H_2SO_4/H_2O); (—) $\mathbf{1}_{ox}H^+$ (pH 0, 1 M HCl); (—) $\mathbf{1}_{ox}$ (pH 8.5, H_2O/KOH); (---) $\mathbf{1}_{ox}^-$ (pH 12.7, H_2O/KOH). Typical concentration employed was 1.5×10^{-5} M.

Scheme I

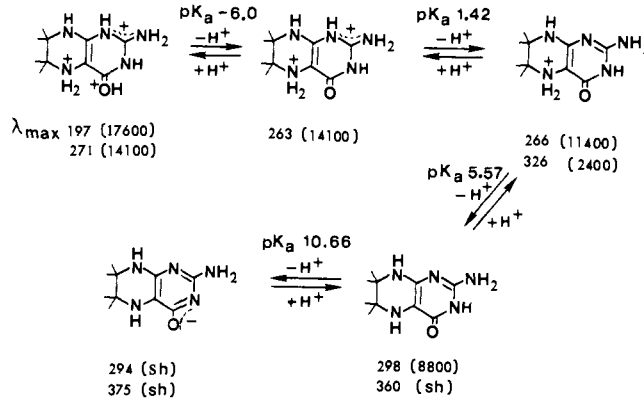

Figure 1. In Scheme I is shown the absorbances of each species and the sites of protonation/deprotonation associated with the various pK_a's. The pK_a's determined for $\mathbf{1}_{red}$ are comparable to those for various other tetrahydropterins (e.g., 1.4, 5.6, 10.4 for 6,7-dimethyl-5,6,7,8-tetrahydropterin[15] and 5.7, 10.65 for 8-methyltetrahydropterin[16]). Upon 2 e^- electrochemical or bromine

(15) Schwotzer, W.; Bieri, J. H.; Viscontini, M.; von Philipsborn, W. *Helv. Chim. Acta* **1978**, *61*, 2108–2115. Kallen, R. G.; Jencks, W. P. *J. Biol. Chem.* **1966**, *241*, 5845–5850.

(16) Pfleiderer, W.; Mengel, R. *Chem. Ber.* **1971**, *104*, 2293–2312.

Scheme II

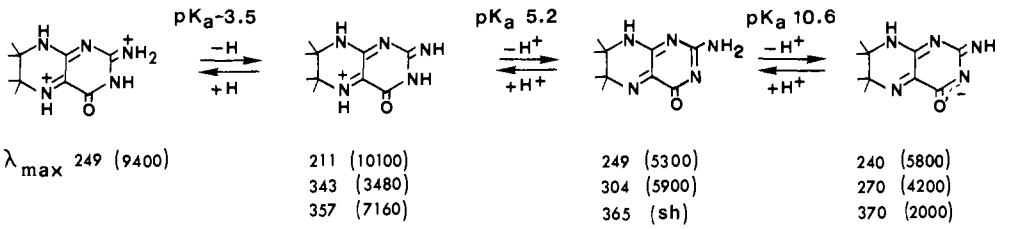

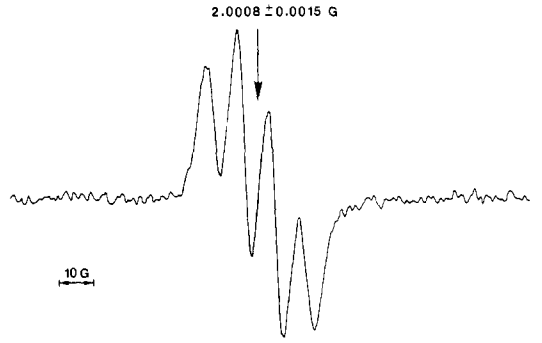

Figure 3. EPR spectrum of $\mathbf{1}_{sem}$ in trifluoroacetic acid. The concentration of radical is 1.27×10^{-5} M. The concentration of $\mathbf{1}_{ox}$ and $\mathbf{1}_{red}$ are 1.5×10^{-2} M.

oxidation of $\mathbf{1}_{red}$ to $\mathbf{1}_{ox}$, the lower pK_a at 1.4 changes to −3.5, while the higher pK_a's remain virtually unchanged. The oxidized 6,6,7,7-tetramethyl-7,8-dihydropterin ($\mathbf{1}_{ox}$) is sufficiently stable to allow studies of its acid–base chemistry. The UV–vis spectra of $\mathbf{1}_{ox}$ at various pH values are shown in Figure 2. The spectrum at pH 8.5 closely resembles the spectrum of the quinonoid 6,7-dimethyl-7,8-dihydropterin prior to its rearrangement to the 7,8-dihydropterin isomer (eq 3).[16] In Scheme II is shown the

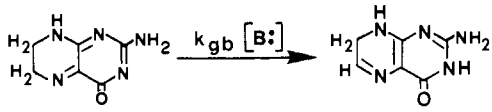

(3)

absorbance of each species of $\mathbf{1}_{ox}$ and the site of protonation/deprotonation associated with each pK_a. The 4-keto-7,8-dihydro exo and endo tautomers of the quinonoid are favored, at acidic and neutral pH, respectively, based on recent ^{15}N NMR studies.[17] However, owing to the possibility of various tautomers, the pK_a's at −3.5 and 5.2 are probably macroscopic.

The semiquinone of 1 ($\mathbf{1}_{sem}$) is obtained on mixing $\mathbf{1}_{red}$ and $\mathbf{1}_{ox}$ in 1 M HCl. If it is assumed that the extinction coefficient of $\mathbf{1}_{sem}$ is 6000 M^{-1} cm^{-1} (approximately the same as for flavin radical[18]), the concentration of $\mathbf{1}_{sem}$ could be calculated as $\sim 6 \times 10^{-7}$ M in a solution initially 10^{-3} M in both $\mathbf{1}_{red}$ and $\mathbf{1}_{ox}$. From this the value of K_e is calculated (eq 4) to be 3.4×10^{-7} M^{-1} (pH 1). This compares well with the equilibrium constant of 7.1×10^{-7} M^{-1} determined by EPR in trifluoroacetic acid. The ESR

$$K_e = [\mathbf{1}_{sem}]^2/[\mathbf{1}_{ox}][\mathbf{1}_{red}] \quad (4)$$

spectrum of $\mathbf{1}_{sem}$ (line width = 4.44 Å) closely resembles the ESR spectra of semiquinones formed from 5-methyl-6,7-diphenyldihydropterin[19] (line width = 4.80 Å) and 5,6,7,8-tetrahydropterin (line width = 5.4 Å).[20] The ESR spectrum for $\mathbf{1}_{sem}$ is centered at $G = 2.0008 \pm 0.0015$ (Figure 3). This is very close to the center for the EPR spectrum of 5,6,7,8-tetrahydropterin radical ($G = 2.003$).[19] Hemmerich et al.[19] concluded from the very favorable comproportionation equilibria of flavin in trifluoroacetic acid that a similar behavior would be observed for pterins. This does not seem to be the case. Formation of pterin radical by comproportionation is far less favorable than is flavin radical formation by comproportionation, since in concentrated trifluoroacetic acid the flavin comproportionation equilibrium constant is >1.

Scheme III

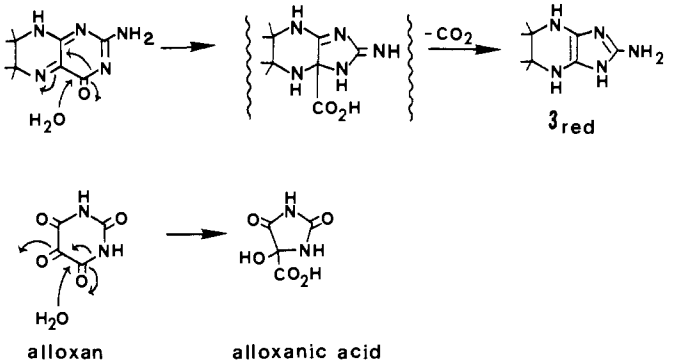

$$\mathbf{1}_{red} + \mathbf{1}_{ox} \underset{k_2}{\overset{k_1}{\rightleftharpoons}} 2\mathbf{1}_{sem} \quad k_1/k_2 = K \quad (5)$$

The quinonoid species rearrange in a general base (k_{gb}[B:]) catalyzed reaction to 7,8-dihydropterins (eq 3).[21] The 6,6-dimethyl-substituted $\mathbf{1}_{ox}$ cannot undergo such an isomerization but instead undergoes a ring contraction followed by decarboxylation that is suggestive of a step in alloxane hydrolysis[22] (Scheme III). Similar ring contractions to yield imidazolones have been recorded for flavin hydrolysis.[23] Since crystalline $\mathbf{1}_{ox}$ forms $\mathbf{1}_{sem}$ in moist air, its conversion to $\mathbf{3}_{red}$ must in turn yield $\mathbf{3}_{ox}$ and $\mathbf{1}_{red}$ via eq 6.

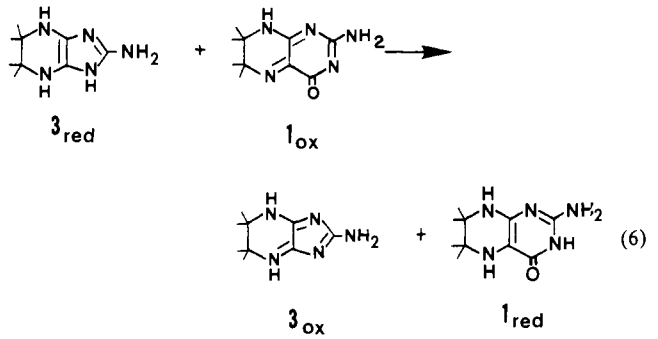

(6)

The latter can react with the remaining $\mathbf{1}_{ox}$ to yield the blue radical $\mathbf{1}_{sem}$. The overall reaction for $\mathbf{1}_{ox}$ in water under anaerobic conditions would then be described by eq 7. $\mathbf{3}_{ox}$ is characterized by its absorbance at 274 nm ($\epsilon \sim 2300$) and the little change in this absorbance upon change in acidity [$H_0 = -0.22$ (1 M $HClO_4$) to pH 6.9, λ_{max} = 270 (21 000)].

$$2\mathbf{1}_{ox} + H_2O \rightarrow \mathbf{1}_{red} + \mathbf{3}_{ox} + CO_2 \quad (7)$$

The synthesis of $\mathbf{2}_{red}$ was accomplished by methylation of $\mathbf{1}_{red}$ with CH_2O by reductive alkylation. That methylation occurred

(17) Armarego, W.; Benkovic, S. J., private communication.
(18) ϵ = 5900 M^{-1} cm^{-1} at 477 nm for 3-acetylethylesterlumiflavin (Ehrenberg, A.; Mueller, F.; Hemmerich, P. *Eur. J. Biochem.* **1967**, *2*, 286–293). ϵ = 4300 M^{-1} cm^{-1} at 500 nm for 5-ethyl-3-methyllumiflavin (Hemmerich, P.; Massey, V.; Michel, H.; Schug, C. In "Structure and Bonding"; Springer: Heidelberg, 1982; Vol. 48).
(19) Ehrenberg, A.; Hemmerich, P.; Mueller, F.; Pfleiderer, W. *Eur. J. Biochem.* **1970**, *16*, 584–591.
(20) Bobst, A. *Helv. Chim. Acta* **1968**, *51*, 607–613.
(21) Archer, M. C.; Scrimgeour, K. G. *Can. J. Biochem.* **1970**, *48*, 278–287.
(22) Van der Plas, H. C. "Ring Transformations of Heterocycles"; Academic Press: New York, 1973; Vol. 2, p 128.
(23) (a) Mager, H. I. X. *Tetrahedron Lett.* **1979**, *26*, 2423–2426. (b) Smith, S. B.; Bruice, T. C. *J. Am. Chem. Soc.* **1975**, *97*, 2875–2881.

Scheme IV

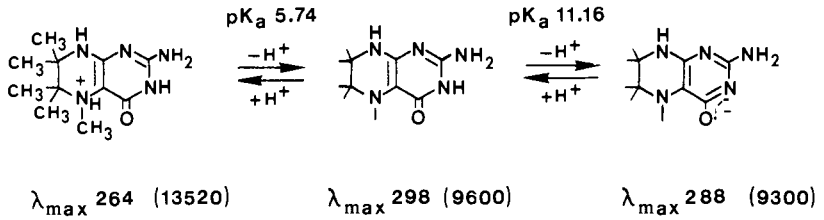

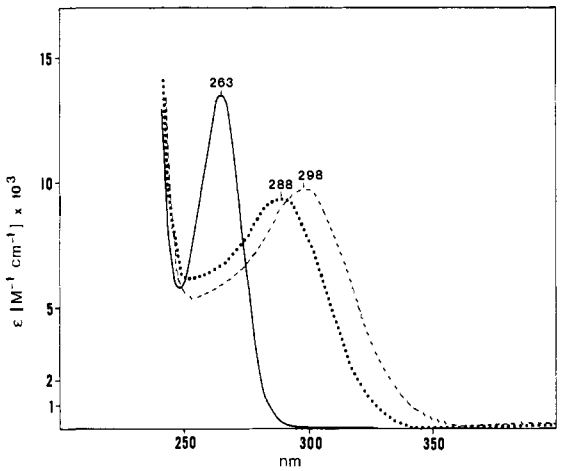

Figure 4. Spectra of the acid–base species of $\mathbf{2}_{red}$. (—) $\mathbf{2}_{red}H^+$ (pH 3.05); (---) $\mathbf{2}_{red}$ (pH 8.35); (···) $\mathbf{2}_{red}^-$ (pH 13.43). The typical concentration employed was 1.5×10^{-5} M.

on the N^5-position of $\mathbf{1}_{red}$ was established by proton NOE measurements (Experimental Section). In analogy to the flavin system, N^5-alkylation of $\mathbf{1}_{red}$ (to yield 5,6,6,7,7-pentamethyl-5,6,7,8-tetrahydropterin ($\mathbf{2}_{red}$)) was anticipated to increase, relative to **1** both the redox potentials and the comproportionation constant for radical formation (eq 8).[15b,21]

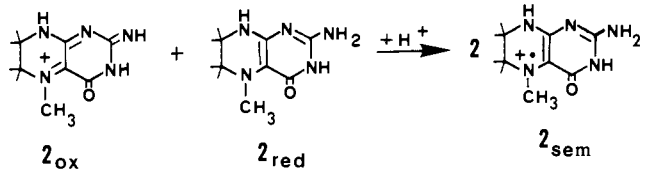

(8)

The Acid–Base Chemistry of $\mathbf{2}_{red}$. The UV–vis spectra of $\mathbf{2}_{red}$ at various pH values are given in Figure 4. N^5-Alkylation does not influence the UV–vis spectra of $\mathbf{2}_{red}$ in comparison to $\mathbf{1}_{red}$ at pH 1 where $\mathbf{1}_{red}$ is protonated on N^5. In Scheme IV is shown the λ_{max} and extinction coefficients for each species of $\mathbf{2}_{red}$ and the sites of protonation/deprotonation with associated pK_a's. The determined pK_a's for $\mathbf{2}_{red}$ compare satisfactorily to those determined for $\mathbf{1}_{red}$.

The compound $\mathbf{2}_{ox}$ is very unstable in water, and its formation and decomposition have only been observed electrochemically (vide infra). $\mathbf{2}_{ox}$ hydrolyzes easily to $\mathbf{1}_{red}$ and HCHO. This facile loss of the N(5)-methyl group is in congruence with the observed (but slower) loss of the N(5)-alkyl substituent of 5-methyllumiflavin,[19] 1,10-ethano-5-ethyllumiflavin,[14a] and derived radicals. The dealkylation of the N(5)-position of $\mathbf{2}_{ox}$ is also related to the quinonoid 7,8-dihydro rearrangement of dihydropteridines.[21] The C(6)-position and the N(5)-methyl group are both susceptible to general base proton removal.[24b]

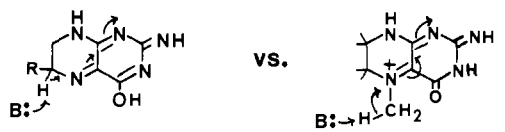

(9)

Scheme V

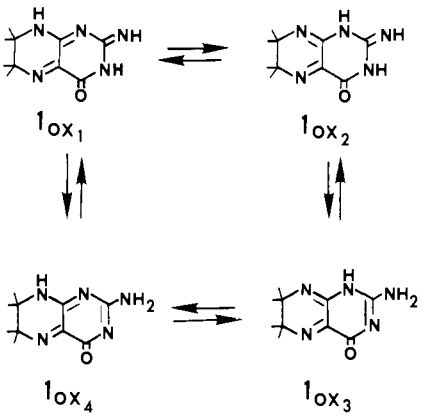

Scheme VI

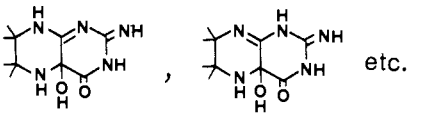

Electrochemistry of 1. The electrochemistry of the interconversion of $\mathbf{1}_{ox}$ and $\mathbf{1}_{red}$ has been studied via the thin-layer CV technique of Hubbard (Figure 5). From the plots of Figure 5 one can compute[13] that a 2 e$^-$ transfer is associated with each oxidation and reduction potential wave at all investigated pH values and that all the 2 e$^-$ transfers are thermodynamically reversible; e.g., <2% of oxidized or reduced **1** decomposes or rearranges irreversibly within the scan time (between 300 to 700 s from the maximum of one peak to the maximum of the counterpeak). Between $H_0 = -4.33$ and pH 2.0 the separation of the oxidation peak and reduction peak is 60 to 90 mV. This indicates that the rate of transfer of electrons at the Pt electrode is almost equally fast toward $\mathbf{1}_{ox}$ and away from $\mathbf{1}_{red}$ and that consecutive reaction must be slow compared to the scan time. Examination of Figure 5 also shows that at $H_0 = -6.6$ the $\mathbf{1}_{ox} \rightarrow \mathbf{1}_{red}$ reduction peak is of "normal" shape and position, whereas the $\mathbf{1}_{red} \rightarrow \mathbf{1}_{ox}$ oxidation peak is greatly broadened and shifted toward a more positive potential. This indicates that the rate of electron transfer to $\mathbf{1}_{ox}$ (eq 10) is greater than the rate constant for electron transfer from $\mathbf{1}_{red}$ to the Pt electrode at this acidity. The rate of the back

$$\mathbf{1}_{ox} + 2e^- \underset{k_{-1}}{\overset{k_1}{\rightleftharpoons}} \mathbf{1}_{red} \qquad (10)$$

reaction is too small in comparison to the scan time (2 mV/s) so that a higher potential is necessary to obtain maximum current. At pH 5.8 to 9.2 electron transfer to $\mathbf{1}_{ox}$ is sluggish while oxidation of $\mathbf{1}_{red}$ is fast. For this reason at pH >5.8 the thin-layer cyclic voltammogram is distorted in a manner just opposite to that seen at $H_0 = -6.6$.

There may be several tautomeric forms of both oxidized and reduced pteridines in equilibrium with each other. For example, the pK_a of $\mathbf{1}_{ox}$ is ~5.2. The following tautomeric equilibria of the neutral $\mathbf{1}_{ox}$ can be considered (Scheme V). For 6-methyldihydropterin, the quinonoid form shown as $\mathbf{1}_{ox4}$ predominates.[17,25]

(24) (a) Hubbard, A. T. *CRC Crit. Rev. Anal. Chem.* **1973**, *3*, 201–242. (b) Kemal, C.; Bruice, T. C. *J. Am. Chem. Soc.* **1976**, *98*, 3955–3964.

(25) Lazarus, R. A.; DeBrosse, C. W.; Benkovic, S. J. *J. Am. Chem. Soc.* **1982**, *104*, 6872–6873.

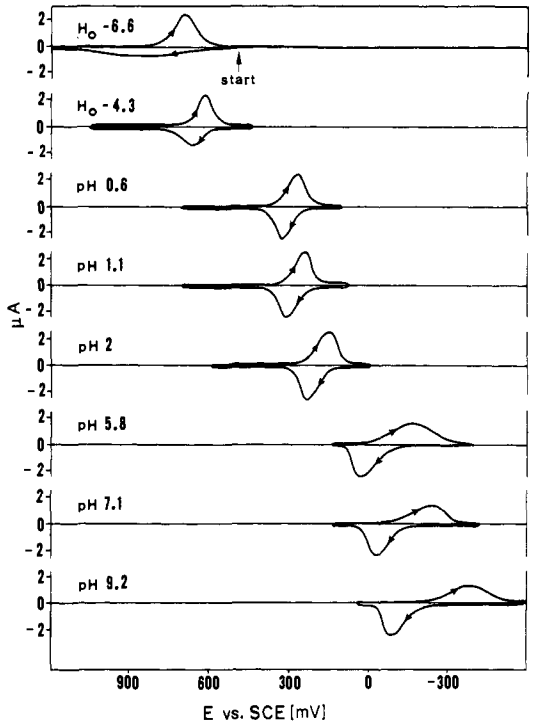

Figure 5. The pH dependence of the thin-layer cyclic voltammogram for **1**, determined at a scan speed of 1 mV/s. The typical concentration employed was 1×10^{-3} M. The initial direction of scan was from negative to positive potential. The area under the curves associated with the peak potentials for anodic and cathodic scans integrate on the average to 1.85 e^-. No indication for 1 e^- transfer is observed.

Consequently the initially reduced $\mathbf{1}_{ox1}$ or $\mathbf{1}_{ox4}$ may rearrange in a tautomeric equilibrium (eq 11). An additional complexity is

$$\mathbf{1}_{ox2} \underset{k_{-3}}{\overset{k_3}{\rightleftharpoons}} \mathbf{1}_{ox1} + 2e^- \underset{k_{-1}}{\overset{k_1}{\rightleftharpoons}} \mathbf{1}_{red1} \underset{k_{-2}}{\overset{k_2}{\rightleftharpoons}} \mathbf{1}_{red2} \qquad (11)$$

where $k_2 > k_{-1} > k_{-2}$ at H_0 -6.6

that one or more of the oxidized forms $\mathbf{1}_{ox1}$, $\mathbf{1}_{ox2}$, $\mathbf{1}_{ox3}$, $\mathbf{1}_{ox4}$ may be in equilibrium with the corresponding 4a-hydrate (Scheme VI), as discussed by Perrin[26] and Pfleiderer.[27]

The redox potentials for stepwise 1 e^- transfer (eq 12 and 13) were not obtained by the applied electrochemical method. From

$$\mathbf{1}_{ox} + 1e^- \rightarrow \mathbf{1}_{sem} \qquad E_1 \qquad (12)$$

$$\mathbf{1}_{sem} + 1e^- \rightarrow \mathbf{1}_{red} \qquad E_2 \qquad (13)$$

the approximated comproportionation equilibrium constant in trifluoroacetic acid of 1 M HCl/H_2O ($K_c = 3 \times 10^{-7}$), the separation of the 1 e^- transfer potentials of eq 12 and 13 ($\Delta E = E_2 - E_1 = (-RT/F) \ln K$) is calculated to be 390 ± 35 mV at pH 1.0. This separation of 1 e^- potentials for the tetramethylpterin system may be compared to the ~20 mV (pH 1.0) and 120 ± 10 mV (pH 7.0) separation of like potentials with riboflavin[28] or lumiflavin.[29] Thus, at like concentrations of reduced and oxidized species radical formation is estimated to be about 100-fold (pH 7.0) or 10^7-fold (pH 1.0) more favorable with flavin as compared to the tetramethylpterin.

In Figure 6A there is presented a Nernst–Clark plot of the 2 e^- redox potential of 6,6,7,7-tetramethylpterin vs. pH. Because the pK_a's for the reduced pterin are almost the same as those for the oxidized pterin, the line does not deviate very much from a constant slope of 60 mV/pH within the observed H_0/pH range. From Figure 6A the standard 2 e^- redox potential $E°$ (eq 10) equals 570 mV and $E°'$ equals 106 mV vs. NHE. As stated

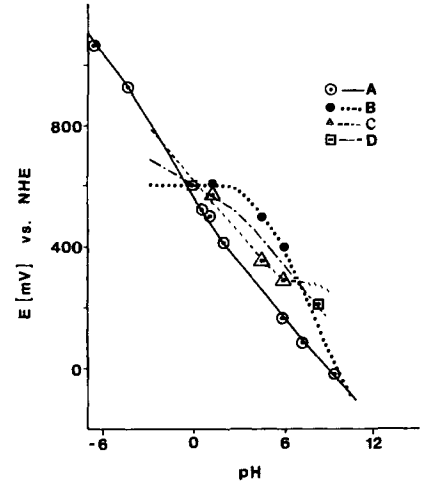

Figure 6. Nernst–Clark plot of potentials vs. pH: (A) 2 e^- reduction of $\mathbf{1}_{ox}$; (B) 1 e^- reduction of $\mathbf{2}_{ox}$; (C) 1 e^- reduction of $\mathbf{2}_{sem}$; (D) 2 e^- reduction of $\mathbf{2}_{ox}$. The points represent experimental values.

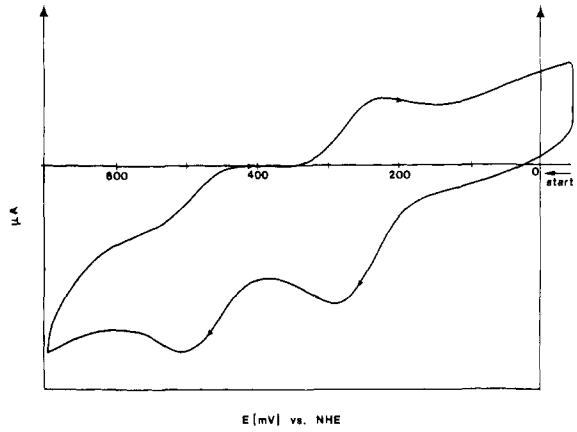

Figure 7. Cyclic voltammogram of **2** at pH 5.9. The initial scan was from negative to positive potential. Scan speed 50 mV/s.

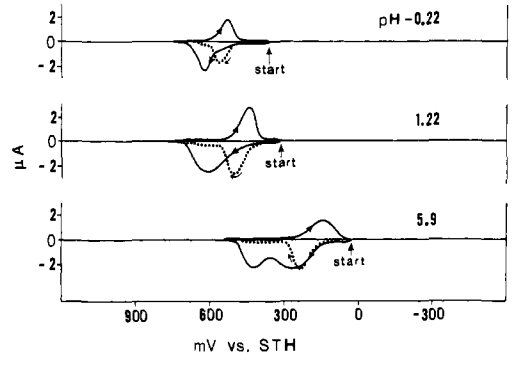

Figure 8. The pH dependence of the thin-layer cyclic voltammogram for **2** determined at a scan speed of 1 mV/s. The typical concentration employed was 1×10^{-3} M. The initial scan direction was from negative to positive potential. Solid line, first scan; dotted line, all consecutive scans.

previously, radical species could not be detected electrochemically within the range of hydrogen ion activities employed (pH 9.2 up to $H_0 = -6.6$).

The literature 2 e^- redox potentials for other pterins are greater than those for **1** by about 35 to 60 mV [$E° = 600$ mV ($E°' = 150$–167 mV)[30,31] for 6,7-dimethylpterin,[25] $E°' = 140$ mV for

(26) Perrin, D. D. *J. Chem. Soc.* **1962**, 645–653.
(27) Pfleiderer, W.; Mengel, R.; Hemmerich, P. *Chem. Ber.* **1971**, *104*, 2273–2292.
(28) Draper, R. D.; Ingraham, L. L. *Arch. Biochem. Biophys.* **1968**, *125*, 802–808.
(29) Lowe, H. J.; Clark, W. M. *J. Biol. Chem.* **1956**, *221*, 983–992.
(30) Archer, M. C.; Von der Schmitt, D. J.; Scrimgeour, K. G. *Can. J. Biochem.* **1972**, *50*, 1174–1182.
(31) Ege-Serpkenci, D.; Dryhurst, G. *Bioelectrochem. Bioenerg.* **1982**, *9*, 175–195.

Scheme VII

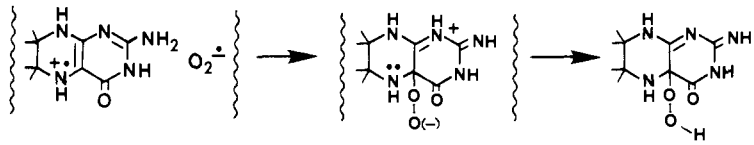

6-methylpterin,[32] $E^{\circ\prime}$ = 150 mV for tetrahydrofolate[33]]. These small differences may be real or artificial. Aside from $\mathbf{1}_{ox}$, the redox reactions are not fully reversible due to rearrangements of the oxidized pterin.[31] The similarity of potentials and pK_a's of 6,6′,7,7′-tetramethylpterin and other pterins makes **1** a suitable molecule for the modeling of pterin reactions.

Electrochemistry of 5,6,6,7,7-Pentamethyltetrahydropterin. Conventional cyclic voltammetry at a scan speed of 50 mV/s with **2** indicates two redox waves (pH 5.6) in both anodic and cathodic directions (Figure 7). The separation of the peak maxima of 57 and 54 mV indicates a 1 e$^-$ transfer step at each potential wave. This conclusion is supported with thin-layer CV (Figure 8) where coulometric calculations can be made. In this instance 1 e$^-$ transfer is seen only when scanning in the anodic direction. Figure 8 shows that $\mathbf{2}_{ox}$ is not sufficiently stable to be detected with the slow scan speeds required for thin-layer CV. When scanning to more positive potential and starting with $\mathbf{2}_{red}$ the oxidation wave at H_0 = −0.22 is only observed in the first scan and is associated with a 3 e$^-$ transfer wave. A reduction wave corresponding to the 3 e$^-$ oxidation is not observed. Instead, further scanning reveals redox waves attributable to **1**. Thus, $\mathbf{2}_{ox}$ is rapidly converted to **1** at H_0 = −0.22. A 1 e$^-$ transfer wave is observed during the electrochemical oxidation of $\mathbf{2}_{red}$ at pH 1.22. No back reduction is observed that corresponds to the 2 e$^-$ oxidation step. Instead, a single 2 e$^-$ transfer wave is observed which corresponds to reduction of $\mathbf{1}_{ox}$. A second scan provides only the single 2 e$^-$ transfer waves characteristic of the thin-layer CV of **1**. At pH 5.9 there are two 1 e$^-$ transfer waves observed for the oxidation of authentic $\mathbf{2}_{red}$ if scanned from negative to positive potential. The first wave from the start is attributed to the electron transfer according to eq 14.

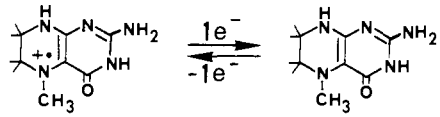

$\mathbf{2}_{sem}$ $\mathbf{2}_{red}$ (14)

The second wave is attributed to the electron transfer according to eq 15. If the electrochemical oxidation of $\mathbf{2}_{red}$ is stopped after the first electron transfer step and the polarity reversed, there is seen a small reduction wave for the radical (the tautomeric form of $\mathbf{2}_{sem}$ is unknown). Repeated thin-layer CV scans between

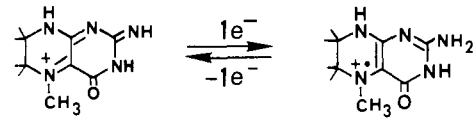

$\mathbf{2}_{ox}$ $\mathbf{2}_{sem}$ (15)

reduced **2** and radical (eq 14) result in a decrease in the 1 e$^-$ oxidation peaks with each scan while a peak for the unalkylated pterin **1** increases. Two isosbestic points are observed (Figure 9). From the time dependency of the disappearance of the reduction wave for the radical, the pseudo-first-order rate constant for the N(5)-dealkylation has been estimated to be 1.4 × 10^{-2} s^{-1} (pH 5.9 with 0.05 M phosphate buffer, μ = 1.0 ($NaClO_4$)).

An approximation of the Nernst–Clark plots for 1 e$^-$ reduction of $\mathbf{2}_{ox}$ (B), 1 e$^-$ reduction of $\mathbf{2}_{sem}$ (C), and 2 e$^-$ reduction of $\mathbf{2}_{ox}$ is included in Figure 6. From these data are calculated: E_1° = 595 ± 10 mV, E_2° = 617 ± 10 mV; and $E_1^{\circ\prime}$ = 260 ± 10 mV, $E_2^{\circ\prime}$ = 280 ± 10 mV.

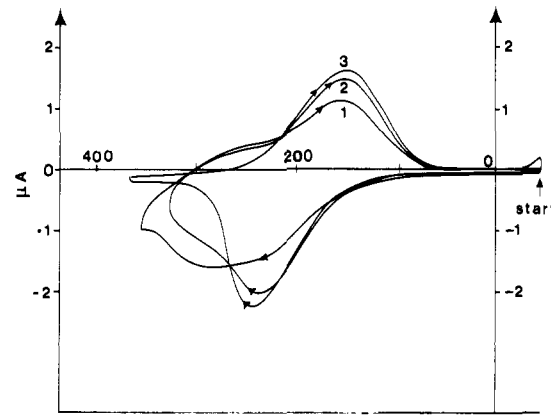

Figure 9. Repeated thin-layer cyclic voltammetric scan for **2** (6.45 × 10^{-4} M) at pH 5.9. This scan is reversed after the radical is formed. The initial scan direction was from negative to positive potential.

Reaction of $\mathbf{1}_{red}$ with O_2 is too slow to follow conveniently at H_0 values below 0. Over the pH range 1 to 11, the reaction is autocatalytic and pH insensitive. From the initial rate constant at pH 1.0 a pseudo-first-order rate constant of 1.6 × 10^{-6} s^{-1} was calcualted so that at an O_2 concentration of 3 × 10^{-4} M the apparent second-order rate constant for reaction of $\mathbf{1}_{red}$ + O_2 is determined as 5 × 10^{-3} M^{-1} s^{-1}. It follows that at pH 1.0, $\Delta G^\ddagger$ = 86 kJ M^{-1}. With a knowledge of the 2 e$^-$ reduction potential of $\mathbf{1}_{ox}$ (eq 17) and the 2 e$^-$ reduction potential of O_2 (eq 16), one calculates (eq 18) the standard (pH 1.0) free energy for 2 e$^-$ reduction of O_2 by $\mathbf{1}_{red}$. At the standard state of 1 M the 2 e$^-$

$$O_2 + 2e^- \rightarrow H_2O_2 \qquad E_m^{pH\ 1.0} = 657\ mV \qquad (16)$$

$$\mathbf{1}_{ox} + 2e^- \rightarrow \mathbf{1}_{red} \qquad E_m^{pH\ 1.0} = 480\ mV \qquad (17)$$

$$\mathbf{1}_{red} + O_2 \rightarrow \mathbf{1}_{ox} + H_2O_2 \qquad emf = 177\ mV \qquad (18)$$

$$\Delta G^\circ = -nF(emf) = -17\ kJ\ M^{-1} \qquad (19)$$

reduction of O_2 by $\mathbf{1}_{red}$ in acid (pH 1) is mildly exothermic. From eq 20[34] and 21 the emf for the 1 e$^-$ transfer from $\mathbf{1}_{red}$ to O_2 can be calculated (eq 22). The standard free energy (ΔG°) at pH

$$O_2 + 1e^- \rightleftharpoons O_2^- \qquad E = -90\ mV\ at\ pH\ 1 \qquad (20)$$

$$\mathbf{1}_{sem} + 1e^- \rightleftharpoons \mathbf{1}_{red} \qquad E = 675 \pm 20\ mV\ at\ pH\ 1 \qquad (21)$$

$$\mathbf{1}_{red} + O_2 \rightleftharpoons \mathbf{1}_{sem} + O_2^- \qquad emf = -765 \pm 20\ mV \qquad (22)$$

1.0 for the reaction of eq 22 is then +74 kJ M^{-1} or highly endergonic. Thus, $\Delta G^\ddagger - \Delta G^\circ$ = 13 kJ M^{-1}. That $\Delta G^\circ < \Delta G^\ddagger$ indicates that the 1 e$^-$ reduction of O_2 by $\mathbf{1}_{red}$ is allowed as a step along the reaction coordinant for reaction of $\mathbf{1}_{red}$ with O_2. In the opposite direction the reduction of $\mathbf{1}_{sem}$ by $O_2^-\cdot$ would then be associated with a diffusion-limited rate constant of 3.6 × 10^{10} M^{-1} s^{-1}. This value is comparable to those computed[14a] for the 1 e$^-$ transfer from $O_2^-\cdot$ to flavin radical. As in the case of dihydroflavin reduction of O_2, the reduction of O_2 by the tetrahydropterin $\mathbf{1}_{red}$ likely involves a 1 e$^-$ transfer step as rate controlling and the transition state resembles closely the $\mathbf{1}_{sem}$–superoxide radical pair. Also, as in the case of dihydroflavin oxidation, $\Delta G^\ddagger$ is virtually

(32) Asahi, Y. *Abh. Deut. Akad. Wiss. Berlin, Kl. Chem., Geol. Biol.* **1964**, *1*, 74.
(33) Kretzschmar, K.; Jaenicke, W. *Z. Naturforsch. B* **1971**, *26*, 225–228.
(34) Calculated with the Nernst equation with data from the following: (a) Rabani, J.; Matheson, M. S. *J. Am. Chem. Soc.* **1964**, *86*, 3175–3176. (b) Koppenol, W. H. *Nature (London)* **1976**, *262*, 420–421. (c) Koppenol, W. H. *Photochem. Photobiol.* **1978**, *28*, 431. (d) George, P. In "Oxidases and Related Redox Systems"; King, T. E., Mason, H. S., Morrison, M., Eds.; Wiley: New York, 1965; Vol. I, p 3.

pH invariant (from pH 1 to 8) so that proton transfer to $O_2^{-}\cdot$ is unlikely. These observations suggest the formation of a 4a-hydroperoxide anion by the coupling of $\mathbf{1}_{sem}$ and $O_2^{-}\cdot$ (Scheme VII).

No H_2O_2 could be detected at completion of the oxidation of $\mathbf{1}_{red}$ by O_2 in aqueous solution so that an overall 4 e^- transfer to oxygen must be assumed. This may occur either through subsequent reaction of the intermediate pterin 4a-hydroperoxide or the H_2O_2 per se (eq 23 and 24 where $k_2 \gg k_1$). In separate

$$\mathbf{1}_{red} + O_2 \xrightarrow{k_1} \mathbf{1}_{ox} + H_2O_2 \quad (23)$$

$$\mathbf{1}_{red} + H_2O_2 \xrightarrow{k_2} \mathbf{1}_{ox} + 2H_2O \quad (24)$$

experiments it was established that $\mathbf{1}_{red}$ is oxidized to $\mathbf{1}_{ox}$ in the presence of H_2O_2. Though 95% of the stoichiometric amount of H_2O_2 can be accounted for on air oxidation of $\mathbf{1}_{red}$ in absolute *tert*-butyl alcohol, the addition of but 3% of water suppresses any H_2O_2 formation in *tert*-butyl alcohol.

The reaction of $\mathbf{2}_{red}$ with O_2 was investigated at pH 4.68 and 8.00. As in the case of $\mathbf{1}_{red}$ oxidation, the reaction is autocatalytic. The second-order rate constants for O_2 oxidation were calculated from initial rates. The values of $\Delta G^{\ddagger}$ were found to be quite similar at both pH values (76 and 71 kJ M^{-1}). The potentials for 1 e^- reduction of $\mathbf{2}_{ox}$ are better known than those in the case of $\mathbf{1}_{ox}$. Calculations such as those detailed for reaction of $\mathbf{1}_{red}$ with O_2 provide $\Delta G°$ of eq 25 as 65 and 58 kJ M^{-1} at pH 4.68 and 8.00.

$$\mathbf{2}_{sem} + O_2^{-}\cdot \rightarrow \mathbf{2}_{red} + O_2 \quad (25)$$

Since $\Delta G^{\ddagger} - \Delta G° = 11$–13 kJ M^{-1}, 1 e^- transfer is allowed to be the rate-limiting step of the reaction of $\mathbf{2}_{red}$ with O_2. As before, the insensitivity of the observed values to pH rules against proton transfer in the rate-limiting step. As found with $\mathbf{1}_{red}$, no H_2O_2 could be detected as a product of the reaction of $\mathbf{2}_{red}$ with O_2 in aqueous solution and $\mathbf{2}_{red}$ was found to be oxidized in the presence of H_2O_2.

The standard free energy for the 4 e^- reduction of oxygen by $\mathbf{1}_{red}$ is determined from the emf of eq 28 to be −64 kJ M^{-1} at pH 6.8. For the oxygen oxidation of $\mathbf{1}_{red}$, reactions according to eq

$$O_2 + 4e^- + 4H^+ \rightarrow 2H_2O \qquad E_m^{pH\ 6.8} + 810\ mV \quad (26)$$

$$\mathbf{1}_{ox} + 2e^- \rightarrow \mathbf{1}_{red} \qquad E_m^{pH\ 6.8} + 150\ mV \quad (27)$$

$$2\mathbf{1}_{red} + O_2 \rightarrow 2\mathbf{1}_{ox} + 2H_2O \qquad emf = 660\ mV \quad (28)$$

22, 29, 30, and 31 may contribute to the observed autocatalysis at pH 6.7. Assuming that $\Delta G^{\ddagger}$ values are directly related to $\Delta G°$

$$\mathbf{1}_{red} + O_2 \rightarrow \mathbf{1}_{sem} + O_2^{-} \qquad \Delta G° = +51\ kJ\ M^{-1};\ k < 2.1\ M^{-1}\ s^{-1} \quad (29)$$

$$\mathbf{1}_{sem} + O_2 \rightarrow \mathbf{1}_{ox} + O_2^{-} \qquad \Delta G° = +39 kJ\ M^{-1};\ k < 503\ M^{-1}\ s^{-1} \quad (30)$$

$$\mathbf{1}_{red} + O_2 \xrightarrow{H^+} \mathbf{1}_{sem} + H_2O_2 \qquad \Delta G° = -110\ kJ\ M^{-1};\ k < 2.2 \times 10^9\ M^{-1}\ s^{-1} \quad (31)$$

values ($\Delta G^{\ddagger} > 20 + \Delta G°$, kJ M^{-1}), it may be concluded that the reactions of eq 30 and 31 would greatly exceed (by $\sim 5 \times 10^2$) in rate the reaction of eq 29. For this reason, autocatalysis involving eq 30 and 31 would intervene in the O_2 oxidation of $\mathbf{1}_{red}$ after only 2% reaction (at 30 °C). The absence of H_2O_2 as a product of their oxidation by O_2 shows that the H_2O_2 oxidation of these reduced species must also be of importance in the autocatalytic reaction. It is interesting to note that the reduction of H_2O_2 is not an important feature in the autocatalytic reaction of O_2 with dihydroflavins. From the emf of eq 32[14a] and 33 (calculated from results of this study) it is obvious that the reductions of H_2O_2 by FlH_2 and by $\mathbf{1}_{red}$ are highly exergonic (−290 and −230 kJ M^{-1}, respectively).

$$FlH_2 + H_2O_2 \rightarrow Fl_{ox} + 2H_2O \qquad emf\ (pH\ 7.0)\ 3.0\ V \quad (32)$$

$$\mathbf{1}_{red} + H_2O_2 \rightarrow \mathbf{1}_{ox} + 2H_2O \qquad emf\ (pH\ 7.0)\ 2.4\ V \quad (33)$$

In conclusion it is interesting to compare the rate of the oxygen reaction with $\mathbf{1}_{red}$ and the turnover of the hydroxylase. At saturating O_2 the pseudo-first-order rate constant for $\mathbf{1}_{red}$ is ca. 10^{-6} s^{-1} whereas turnover of the phenylalanine hydroxylase is ca. 10 s^{-1} or a rate enhancement factor of 10^7. Consequently roles for the enzyme's nonheme iron may include its binding of oxygen as well as its catalysis of oxygen addition to the pterin. The latter presupposes that the pterin hydroperoxide is on the pathway for hydroxylation, a tenet as yet unproven. Consequently, the reactions of $\mathbf{1}_{ox}$ and $\mathbf{1}_{red}$ with H_2O_2 are under investigation.

Acknowledgment. This work was supported by grants to T.C.B. from the National Institutes of Health and to S.J.B. from the National Science Foundation.